NNLO Corrections to the Polarized Drell-Yan Coefficient Function.

V. Ravindran,[a*] J. Smith,[b] W.L. van Neerven.[c]

[a]Harish-Chandra Research Institute, Chhatnag Road, Jhusii, Allahabad, 211019, India.

[b]C.N. Yang Institute for Theoretical Physics, State University of New York at Stony Brook, New York 11794-3840, USA

[c]Instituut-Lorentz, Universiteit Leiden, PO Box 9506, 2300 RA Leiden, The Netherlands.

We present the full next-to-next-to-leading order (NNLO) corrections to the coefficient function for the polarized cross section $d\,\Delta\sigma/d\,Q$ of the Drell-Yan process. We study the effect of these corrections on the process $p+p \to l^+l^- + `X'$ at an C.M. energy $\sqrt{S} = 200$ GeV. All QCD partonic subprocesses have been included provided the lepton pair is created by a virtual photon, which is a valid approximation for a lepton pair invariant mass $Q < 50$ GeV. For this reaction the dominant subprocess is given by $q + \bar{q} \to \gamma^* + `X'$ and its higher order corrections so that it provides us with an excellent tool to measure the polarized sea-quark densities.

1. Introduction

Deep inelastic electroproduction is very useful to extract information about the polarized valence parton densities Δu_v and Δd_v. However almost no information exists about the gluon density Δg and the sea-quark densities Δu_s, Δd_s and Δs (including the anti-sea-quark densities). One of the processes proposed to measure the latter densities is the Drell-Yan process or massive lepton pair production $p + p \to l^+l^- + `X'$. In this reaction the dominant subprocess is given by valence-quark sea-quark annihilation into the lepton pair which continues to hold if we include higher order QCD corrections. Lepton pair production is given by the process

$$p(P_1,S_1) + p(P_2,S_2) \to \gamma^*(q) +' X' \,. \\ \qquad\qquad\qquad\qquad\qquad | \\ \qquad\qquad\qquad\qquad\qquad \to l^+(l_1) + l^-(l_2)$$

$$S = (P_1 + P_2)^2 \,, \quad Q^2 \equiv q^2 = (l_1 + l_2)^2 \,, \quad (1)$$

In the frame work of the parton model this process is described by the Drell-Yan mechanism where the protons are longitudinally polarized. At $\sqrt{S} = 200$ GeV the photon dominates which

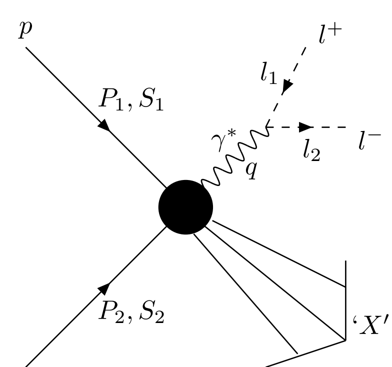

Figure 1. Massive lepton pair production $p+p \to \gamma^* + `X'$.

*Deutsches Elektronen-Synchroton DESY, Platanenallee 6, 15738 Zeuthen.

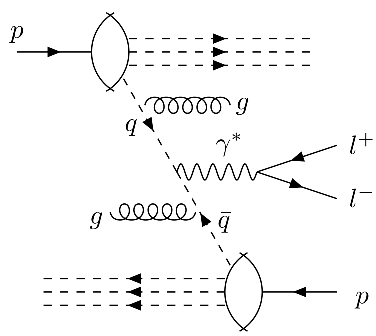

Figure 2. The Drell-Yan process for $p + p \rightarrow \gamma^* + `X'$.

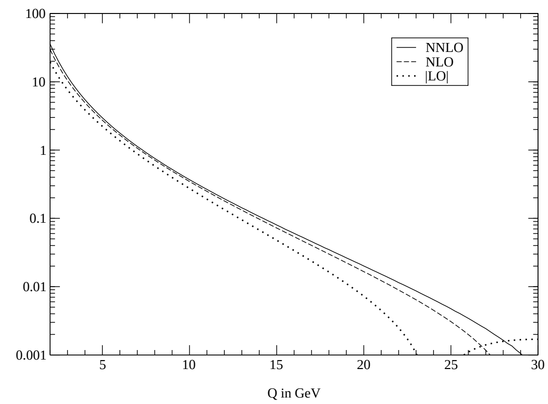

Figure 3. The cros section $d\Delta\sigma/dQ$ in pb/GeV plotted in the range $2 < Q < 30$ GeV at $\mu = Q$ in LO, NLO and NNLO.

is characteristic of the RHIC energies at BNL. Let us first look at the transverse momentum p_T and rapidity y distributions. They are given by

$$S\,\frac{d^3\,\Delta\sigma}{dQ^2\,dp_T\,dy} = \frac{4\,\pi\,\alpha^2}{3\,N_C\,Q^2}\,\frac{d^2\,\Delta W}{dp_T\,dy}\,, \tag{2}$$

where N_C denotes the number of colours. In the QCD improved parton model we have

$$\frac{d^2\,\Delta W}{dp_T\,dy} = \sum_{a_1,a_2=q,g}\int dx_1\int dx_2\,\Delta f_{a_1}(x_1,\mu^2)$$
$$\times\Delta f_{a_2}(x_2,\mu^2)\,\frac{d^2\,\Delta\hat{W}_{a_1a_2}}{dp_T\,dy}\,, \tag{3}$$

where the factorization/renormalization scale is μ^2 and Δf_{a_1} is the polarized parton density. The NLO corrections to the partonic distribution $d^2\,\Delta\hat{W}_{a_1a_2}/dp_T\,dy$ have been completely calculated in [1] (for the non-singlet part see also [2]). For $p_T > Q/2$ the $O(\alpha_s)$ quark-gluon subprocess dominates over all other reactions provided there is a substantial gluon density. Therefore a measurement of the differential p_T distribution is sensitive to the polarized gluon density. This is revealed by the the longitudinal asymmetry $A_{LL} = \Delta\sigma/\sigma$ where the set with the largest gluon density leads to the largest asymmetry.

2. Computational details

A different picture is shown by the invariant mass squared distribution given by

$$\frac{d\,\Delta\sigma}{dQ^2} = \frac{4\,\pi\,\alpha^2}{3\,N_C\,Q^2\,S}\,\Delta W\left(\tau,\frac{Q^2}{\mu^2}\right)\,, \quad \tau = \frac{Q^2}{S}\,. \tag{4}$$

The structure function ΔW equals

$$\Delta W\left(\tau,\frac{Q^2}{\mu^2}\right) = \sum_{a_1,a_2=q,g}\int_\tau^1 dx_1\int_{\tau/x_1}^1 dx_2$$
$$\times\Delta f_{a_1}(x_1,\mu^2)\,\Delta f_{a_2}(x_2,\mu^2)$$
$$\times\Delta_{a_1a_2}\left(\tau,\frac{Q^2}{\mu^2}\right)\,. \tag{5}$$

Here the zeroth order quark-anti-quark process dominates so that this process is an excellent tool to measure the sea-quark density in proton-proton reactions. The NLO corrections to the coefficient function $\Delta_{a_1a_2}$ were calculated in [3] and the NNLO corrections have been recently computed in [4]. In higher order the quark-anti-quark process also dominates. If $\tilde{M}$ is the amplitude of a parton-parton subprocess then the $q\bar{q}$ is given by

$$q(p_1,s_1) + \bar{q}(p_2,s_2) \rightarrow \gamma^* +' X'\,,$$

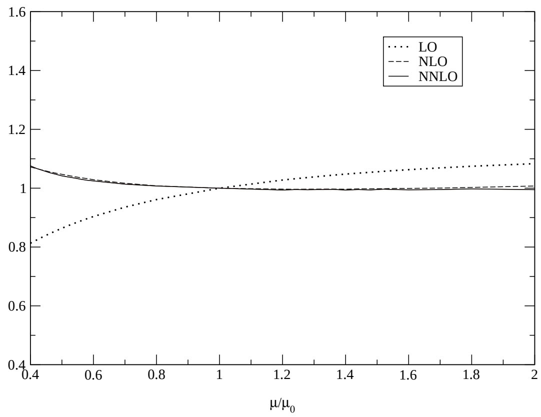

Figure 4. The polarized quantity $N(\mu/\mu_0)$ plotted in the range $0.4 < \mu/\mu_0 < 2$ with $Q = 5$ GeV and $\mu_0 = Q$.

$$|\Delta M_{q\bar{q}}|^2 = \frac{1}{4}\,\mathbf{Tr}\,\Big(\gamma_5 \not{s}_2\,(\not{p}_2 - m)\,\tilde{M}\,\gamma_5 \not{s}_1 \times (\not{p}_1 + m)\tilde{M}^\dagger\Big)\,, \qquad (6)$$

$q_1(\bar{q}_1)(p_1, s_1) + g(p_2) \to \gamma^* +' X'$,

$$|\Delta M_{qg}|^2 = \frac{1}{4}\,\epsilon_{\mu\nu\lambda\sigma}\,\frac{p_2^\lambda\, l_2^\sigma}{p_2 \cdot l_2}\,\mathbf{Tr}\,\Big(\tilde{M}^\mu\,\gamma_5 \not{s}_1 \times (\not{p}_1 \pm m)\,\tilde{M}^{\nu\dagger}\Big)\,, \qquad (7)$$

$q_1(\bar{q}_1)(p_1, s_1) + q_2(\bar{q}_2)(p_2, s_2) \to \gamma^* +' X'$

$$|\Delta M_{q_1 q_2}|^2 = \frac{1}{4}\,\mathbf{Tr}\,\Big(\gamma_5 \not{s}_2\,(\not{p}_2 \pm m)\,\tilde{M}\,\gamma_5 \not{s}_1 \times (\not{p}_1 \pm m)\,\tilde{M}^\dagger\Big)\,, \qquad (8)$$

$g(p_1) + g(p_2) \to \gamma^* +' X'$,

$$|\Delta M_{gg}|^2 = \frac{1}{4}\,\epsilon_{\mu_2\nu_2\lambda_2\sigma_2}\,\frac{p_2^{\lambda_2}\, l_2^{\sigma_2}}{p_2 \cdot l_2}\,\epsilon_{\mu_1\nu_1\lambda_1\sigma_1} \times \frac{p_1^{\lambda_1}\, l_1^{\sigma_1}}{p_1 \cdot l_1}\,\mathbf{Tr}\,\Big(\tilde{M}^{\mu_1\mu_2}\,\tilde{M}^{\nu_1\nu_2\dagger}\Big)\,, \qquad (9)$$

with the constraints

$$s_i \cdot p_i = 0\,, \quad s_i \cdot s_i = -1\,, \quad l_i \cdot l_i = 0\,. \qquad (10)$$

All these reactions contain the γ_5-matrix and/or the Levi-Civita tensor. If we use n-dimensional regularization we have to find a prescription for these typical four dimensional objects. Here we choose the prescription of HVBM [5] or equivalently the one given by [6]. Choosing the latter we obtain the prescription

1. Replace the γ_5-matrix by
$$\gamma_\mu\,\gamma_5 = \frac{i}{6}\,\epsilon_{\mu\rho\sigma\tau}\,\gamma^\rho\,\gamma^\sigma\,\gamma^\tau \quad \text{or}$$
$$\gamma_5 = \frac{i}{24}\,\epsilon_{\rho\sigma\tau\kappa}\,\gamma^\rho\,\gamma^\sigma\,\gamma^\tau\,\gamma^\kappa\,.$$

2. Compute all matrix elements in n dimensions.

3. Evaluate all Feynman integrals and phase space integrals in n-dimensions.

4. Contract the Levi-Civita tensors in four dimensions after the Feynman integrals and phase space integrals are carried out.

This procedure requires an intensive tensorial reduction of the loop-integrals as well as the phase space integrals. However the HVBM methods entails the presence of evanescent counter terms. They were calculated up to two-loop order in [7]. The result has the following structure

$$Z_{qq}^{5,\mathrm{NS},+} = \delta(1-x) + a_s\,S_\varepsilon\,\left(\frac{Q^2}{\mu^2}\right)^{\varepsilon/2}\,\Big[z_{qq}^{(1)} + \varepsilon\bar{z}_{qq}^{(1)}\Big] + \hat{a}_s^2\,S_\varepsilon^2\,\left(\frac{Q^2}{\mu^2}\right)^{\varepsilon} \times\left[+\frac{1}{\varepsilon}\,\beta_0\,z_{qq}^{(1)} + z_{qq}^{(2),\mathrm{NS},+}\right]\,, \qquad (11)$$

where $a_s = \alpha_s(\mu^2)/4\pi$ is the renormalized coupling constant. Further $\bar{z}_{qq}^{(1)}$ and $(Q^2/\mu^2)^{k\varepsilon}$ are

process dependent. The other constants are process independent. The latter also holds for the following pieces

$$Z_{qq}^{5,\mathrm{NS},-} = -\hat{a}_s^2\, S_\varepsilon^2 \left(\frac{Q^2}{\mu^2}\right)^\varepsilon \left[z_{qq}^{(2),\mathrm{NS},-}\right], \tag{12}$$

$$Z_{qq}^{5,\mathrm{PS}} = \hat{a}_s^2\, S_\varepsilon^2 \left(\frac{Q^2}{\mu^2}\right)^\varepsilon \left[z_{qq}^{(2),\mathrm{PS}}\right], \tag{13}$$

The constant $Z_{qq}^{5,\mathrm{NS},+}$ is chosen in such a way that the following relation holds

$$\left(Z_{qq}^{5,\mathrm{NS},+}\right)^2 = -\frac{\Delta\hat{W}_{q\bar{q}}^{\mathrm{NS}}(\hat{a}_s, Q^2/\mu^2)}{\hat{W}_{q\bar{q}}^{\mathrm{NS}}(\hat{a}_s, Q^2/\mu^2)} \tag{14}$$

where $\hat{W}_{q\bar{q}}^{\mathrm{NS}}$ is the partonic structure function of the unpolarized reaction. We have to remove the spurious terms coming from the γ_5 and Levi-Civita prescription in the partonic structure function by using these evanescent counter terms. Since they are present in the (anti-)quark sector we have to form the following products

$$\left(Z_{qq}^5\right)^{-2} \Delta W_{q\bar{q}}\,, \quad \left(Z_{qq}^5\right)^{-1} \Delta W_{qg}\,,$$
$$\left(Z_{qq}^5\right)^{-2} \Delta W_{qq}\,, \quad \Delta W_{gg} \tag{15}$$

3. Results

The processes which have to be calculated up to NNLO are

$$q + \bar{q} \to \gamma^*\,. \tag{16}$$

$$q + \bar{q} \to \gamma^* + g\,, \tag{17}$$

$$g + q(\bar{q}) \to \gamma^* + q(\bar{q})\,. \tag{18}$$

$$q + \bar{q} \to \gamma^* + g + g\,, \tag{19}$$

$$g + q(\bar{q}) \to \gamma^* + q(\bar{q}) + g\,, \tag{20}$$

$$q + \bar{q} \to \gamma^* + q + \bar{q}\,, \tag{21}$$

$$q(\bar{q}) + q(\bar{q}) \to \gamma^* + q(\bar{q}) + q(\bar{q})\,, \tag{22}$$

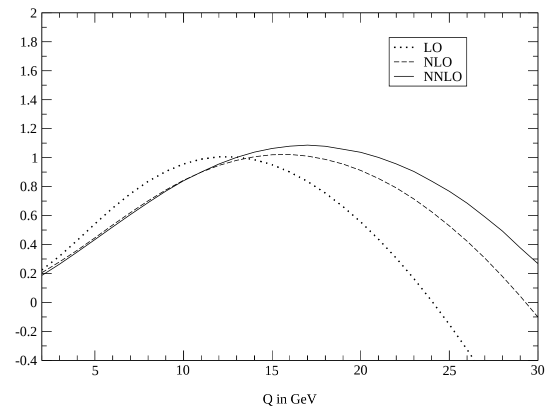

Figure 5. The longitudinal asymmetry A_{LL} plotted in percent in the range $2 < Q < 30$ GeV at $\mu = Q$ in LO, NLO and NNLO.

$$g + g \to \gamma^* + q + \bar{q}\,. \tag{23}$$

including virtual corrections to lower order processes. Apart from evanescent counter terms which are characteristic of the γ_5 and Levi-Civita prescription the calculation proceeds in the same way as in the unpolarized case. The renormalization and mass factorization are carried out in the $\overline{MS}$-scheme. We use the BB1 [8] parton density set to make our plots. The figures are constructed as follows

LO	$\Delta f^{LO}(x,\mu^2)$	α_s^{LO}
NLO	$\Delta f^{NLO}(x,\mu^2)$	α_s^{NLO}
$NNLO$	$\Delta f^{NLO}(x,\mu^2)$	α_s^{NLO}

Because of the lack of the three-loop anomalous dimensions we have no Δf^{NNLO}. Therefore in NNLO we use the NLO parton density set and the two-loop corrected running coupling constant α_s^{NLO}. Further we set the mass factorization scale equal to the renormalization scale unless stated otherwise. Since we also compare with the unpolarized Drell-Yan process we choose the following parton density sets given by [9]. Since they have an approximate NNLO set we plot the figures according to

$LO \qquad f^{LO}(x,\mu^2) \qquad \alpha_s^{LO}$

$NLO \qquad f^{NLO}(x,\mu^2) \qquad \alpha_s^{NLO}$

$NNLO \qquad f^{NNLO}(x,\mu^2) \qquad \alpha_s^{NNLO}$

Our findings are that the quark-anti-quark channel dominates the proton-proton reaction in polarized as well as well in unpolarized physics. The invariant mass distribution is shown in Fig. 3 in LO, NLO and NNLO. The K-factors defined by

$$K^{(i)} = \frac{\sigma^{(i)}}{\sigma^{LO}}\,, \qquad \Delta K^{(i)} = \frac{\Delta\,\sigma^{(i)}}{\Delta\,\sigma^{LO}}\,, \tag{24}$$

are roughly the same. For $Q = 7$ GeV at $\sqrt{S} = 200$ GeV we get a minimum. Here the values are $\Delta K^{NLO} = 1.2$ and $\Delta K^{NNLO} = 1.3$ respectively. In Fig. 4 we have plotted for $Q = 5$ GeV the mass factorization scale dependence

$$N\left(\frac{\mu}{\mu_0}\right) = \frac{\Delta\sigma(\mu)}{\Delta\sigma(\mu_0)}\,, \tag{25}$$

for $\mu_0 = Q$ and $0.4\,\mu_0 < \mu < 2\,\mu_0$. We see a clear improvement while going from LO to NLO and surprisingly also from NLO to NNLO. In Fig. 5 we have shown the longitudinal asymmetry

$$A_{LL} = \frac{\Delta\,\sigma}{\sigma}\,, \tag{26}$$

in LO, NLO and NNLO. To compare the different polarized parton densities we have also plotted in Fig.6 the longitudinal asymmetry for the BB2 [8] and the GRSV standard (SS) and valence (VS) parametrizations [10]. The figure reveals that the largest gluon (BB1) leads to smallest asymmetry. On the other hand the smallest gluon (VS) gives the largest asymmetry. Notice that the latter parametrization produces the smallest asymmetry in the differential p_T-distribution.

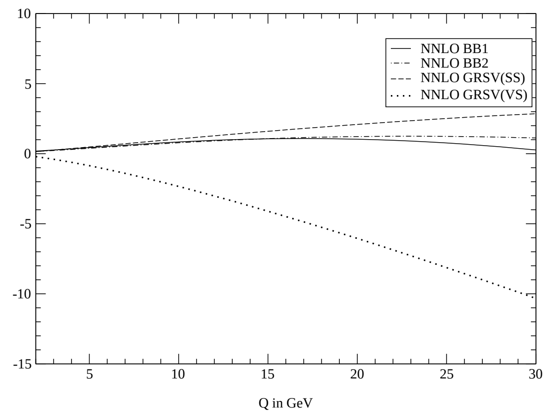

Figure 6. The longitudinal asymmetry A_{LL} plotted in percent in the range $2 < Q < 30$ GeV at $\mu = Q$ and NNLO.

REFERENCES

1. V. Ravindran, J. Smith, W.L. van Neerven, Nucl. Phys. B647 (2002) 275.
2. S. Chang, C. Coriano, R.D. Field, L.E. Gordon, Nucl. Phys. B512 (1998) 393.
3. P.G. Ratcliffe, Nucl. Phys. B223 (1983) 45.
4. V. Ravindran, J. Smith, W.L. van Neerven, Nucl. Phys. B682 (2004) 421.
5. G. 't Hooft and M. Veltman, Nucl. Phys. **B44** (1972) 189;
   P. Breitenlohner and B. Maison, Commun. Math. **53** (1977) 11, 39, 55.
6. D. Akyeampong and R. Delbourgo, Nuov. Cim. **17A** (1973) 578, **18A** (1973) 94, **19A** (1974) 219.
7. Y. Matiounine, J. Smith, W.L. van Neerven, Phys. Rev. D58 (1998) 076002.
8. J. Blumlein, H. Böttcher, Nucl. Phys. B636 (2002) 225.
9. A.D. Martin, R.G. Roberts, W.J. Stirling, R.S. Thorne, Phys. Lett. B531 (2002) 216; Eur. Phys. J. C23 (2002) 73.
10. M. Glück, E. Reya, M. Stratmann, W. Vogelsang, Phys. Rev. D63 (2001) 094005.